briefly described (details are available in reference 5). Air was the working fluid. The test section consisted of a 4-in. diameter outer tube and a series of three interchangeable inner tubes. The resulting duct radius ratios were $r_1/r_2 = 0.28$, 0.56, and 0.75. Any value of the eccentricity ϕ could be attained by adjusting the position of the inner tube. The test section was oriented vertically to eliminate the possibility of sag.

The velocity profiles were sensed by a total pressure probe mounted on a traversing mechanism which permitted carefully controlled travel normal to either tube at various angular positions. After the velocity distribution had been measured, constant velocity lines were drawn on a layout of the duct cross section. Then, zero shear lines (that is, gradient lines) were constructed perpendicular to the constant velocity lines. Once such a contour diagram had been completed, the local wall shear stress was found by making a force balance on a control surface composed of gradient lines and the wall. By this technique, the wall shear stress distribution was obtained for the aforementioned radius ratios and for several eccentricities. It was found that the normalized wall shear stress distribution was essentially independent of Reynolds number in the range from 30,000 to 180,000.

The experimental data just described are plotted in Figure 1. At the higher radius ratios, the agreement between the laminar theory and the turbulent data is remarkably good, for the lowest radius ratio, $r_1/r_2 = 0.25$, the agreement is not quite as good. However, the data themselves may contain uncertainties owing to the possible existence of a secondary flow in the cross section. The departure between the laminar and turbulent results at smaller values of r_1/r_2 is consistent with the findings of Brighton and Jones (*6*) for the concentric annulus.

NOTATION

e = distance between centers
f = friction factor
N_{Re} = Reynolds number
p = static pressure
$\bar{u}$ = average velocity
z = axial coordinate

Greek Letters

θ = angular coordinate
μ = dynamic viscosity
ρ = density
τ = local wall shear
$\bar{\tau}$ = average wall shear
ϕ = eccentricity

Subscripts

1 = inner wall
2 = outer wall

LITERATURE CITED

1. Snyder, W. T., and G. A. Goldstein, *A.I.Ch.E. J.*, **11**, 462 (1965).
2. Caldwell, A., *J. Roy. Tech. Coll. Glasgow*, **2** (1930).
3. Piercy, N. A. V., M. S. Hooper, and H. F. Winny, *Phil. Mag. Ser. 7*, **15**, 617 (1933).
4. Dryden, H. L., F. D. Murnaghan, and Harry Bateman, "Hydrodynamics," p. 198, Dover, New York (1956).
5. Jonsson, V. K., Ph.D. thesis, Univ. Minnesota, Minneapolis (1965).
6. Brighton, J. A., and J. B. Jones, *J. Basic Eng.*, **D86**, 835 (1964).

Nonequilibrium, Inverse Temperature Profile in Boiling Liquid-Metal Two-Phase Flow

JOHN C. CHEN

Brookhaven National Laboratory, Upton, New York

The results of recent experiments with boiling two-phase flow of potassium indicate the existence of an inverse temperature profile in the two-phase fluid. This note presents some of the results and a theoretical explanation for this phenomenon.

EXPERIMENT

Wall and fluid temperatures were measured for vertical axial flow of potassium vapor and liquid through a boiling section. As shown in Figure 1, twelve thermocouples were used to measure temperatures at various radial positions in the boiler wall, and three immersion thermocouples located at the axis of the pipe were used to measure the fluid temperature. The test section was installed in a pumped loop which supplied potassium vapor-liquid mixtures at controlled temperatures, pressure, flow rates, and qualities.

Figure 2 shows temperature data collected for three sample boiling runs. Temperatures measured in the wall and in the fluid are plotted against the log of the radial position. Runs B-12b and B-9b represent the "normal" situation where the I.D. wall temperature is higher than the fluid temperature. Run B-11b represents the unexpected situation where the wall temperature is lower than the fluid center line temperature. This inverse temperature profile actually was found for a majority of the runs in this particular series of tests. The range of variables covered in the test were: flow rate—0.9 to 4.9 gpm, potassium temperature—1,510° to 1,650°F., boiling pressure—28 to 42 lb./sq. in. abs., vapor quality—0.7 to 17.0%, and boiling heat flux—10,200 to 81,700 B.t.u./(hr) (sq. ft.) The measured difference between I.D. wall temperature and fluid core temperature ($T_w - T_o$) ranged from +4.2° to −9°F.

The runs with negative temperature differences were first thought to be in error, but repeated checks of the experi-

(*Continued from page 1144*)

Entrance region flow, Christiansen, E. B., and H. E. Lemmon, **A.I.Ch.E. Journal, 11,** No. 6, p. 995 (November, 1965).

Key Words: A. Flow-8, Fluids-9, Newtonian-0, Entrance-9, Tube-9, Circular-0, Calculation-8, Velocity Profiles-2, Entrance Lengths-2, Pressure Gradient-2, Theoretical-0, Experimental-0, Isothermal-0, Laminar-0, Equations of Motion-1, Fluid Dynamics-8, Design-4, Pipelines-9.

Abstract: The results of rigorous numerical solutions of the general equations of motion are presented for isothermal, laminar, Newtonian flow in a tube entrance region for a uniform entrance velocity. Computed velocity profiles, entrance lengths, and pressure gradients are compared with previous theoretical and experimental results.

Dimensional analysis in photochemical reactor design, Dolan, William J., Carl A. Dimon, and Joshua S. Dranoff, **A.I.Ch.E. Journal, 11,** No. 6, p. 1000 (November, 1965).

Key Words: A. Design-8, Reactors-9, Photochemical-0, Scale-Up-8, Partial Differential Equations-10, Tubes-10, Performance-8, Decomposition-8, Hexachlorophlatinic Acid-1, Water-1, Ultraviolet Light-10.

Abstract: This work is part of a research program on photochemical reactor design and scale-up. The approach taken in this study was to formulate the partial differential equations which describe a continuous tubular photochemical reactor and to extract from the dimensionless form of these equations the dimensionless groups upon which reactor performance should depend.

Diffusion through the liquid-liquid interface: Part II. Interfacial resistance in three-component systems, Ward, W. J., and J. A. Quinn, **A.I.Ch.E. Journal, 11,** No. 6, p. 1005 (November, 1965).

Key Words: Diffusion-8, Liquid-Liquid Interface-9, Acetic Acid-1, Benzoic Acid-1, Oleic Acid-1, Cholesterol-1, Benzene-5, Acids (Carboxylic)-1, Aromatic Hydrocarbons-5, Water-5, Jets-10, Resistance-8, Interface-9, Mass Transfer-8, Equilibrium-8, Contact Time-8, Solubility-8.

Abstract: The transfer of solute molecules across the liquid-liquid interface has been investigated. Measurements are reported on the transfer of acetic acid, benzoic acid, oleic acid, and cholesterol between benzene and water. Experiments were carried out with a laminar jet apparatus wherein the organic phase is spread as a thin film on the surface of an aqueous jet. The results indicate that any interfacial resistance in these systems is negligibly small.

Effective wall heat transfer coefficients and thermal resistances in mathematical models of packed beds, Crider, J. E., and A. S. Foss, **A.I.Ch.E. Journal, 11,** No. 6, p. 1012 (November, 1965).

Key Words: A. Heat Transfer-8, Heat Transfer Coefficient-8, Packed Beds-9, One-Dimensional Model-10, Finite Stage Model-10, Mathematical Model-10, Thermal Resistance-8.

Abstract: Expressions are derived for an effective wall heat transfer coefficient useful in one-dimensional representations of heat transport in packed beds. These expressions are obtained with two mathematical models of a cylindrical packed bed: A partial differential model and a finite stage model. For each model, an approximate expression for the effective thermal resistance of the bed is found that is useful in estimations of heat transfer coefficients.

(*Continued on page 1148*)

mental method and equipment served only to verify the phenomenon. Heat fluxes calculated from the slope of the temperature gradient in the wall were in agreement with input power measurements. Repeated thermocouple calibrations made no apparent difference. With the large number of thermocouples used in determining the wall temperatures, the degree of uncertainty in the extrapolated I.D. wall temperature was much smaller than the negative temperature differences obtained. Most important, runs with *single* phase flow gave *positive* temperature differences of up to 30°F., as expected. The measured single-phase Nusselt numbers agreed with the recent data of Baker and Sesonske (*1*) and with the theoretical predictions of Dwyer (*2*).

It was finally concluded that the observed negative temperature differences represent a true phenomenon.

THEORY

All the runs with negative temperature differences were in the quality range of 9 to 17%. At the test pressures, two-phase flow of this quality would be of the annular type where the vapor flows in a central core (with varying amounts of entrainment) and the liquid flows in an annular film on the pipe wall. Figure 3*a* shows the postulated radial temperature profile for cases where a negative temperature difference exists. With net heat input there must be a temperature drop through the liquid film to a vapor-liquid interface temperature which would be close to, or equal to, the saturation temperature T_s. It is often assumed that the vapor temperature in the core stays approximately constant at the saturation temperature throughout the vapor

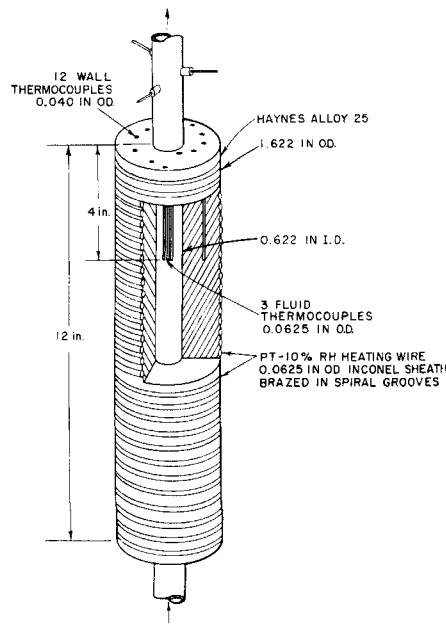

Fig. 1. Boiling test section.

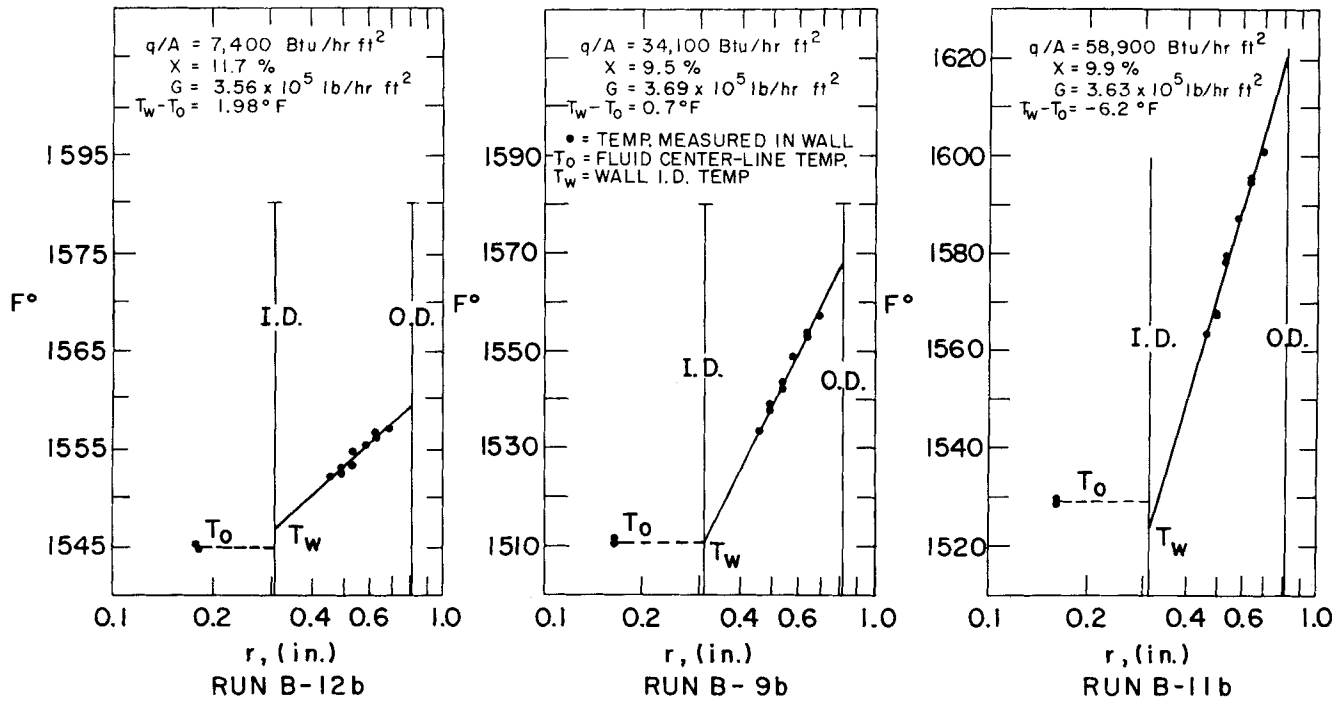

Fig. 2. Temperature profiles measured in test section.

cross section, as shown by the dotted line in Figure 3*a*. However, since the measured core temperature T_o is higher than the I.D. wall temperature, the profile must then necessarily invert and rise from the value T_s at the interface to the value T_o at the center line of the vapor core. This implies that the vapor core exists in a superheated state relative to the local pressure. The question is, then, what is the mechanism causing the vapor core to be at this higher temperature, nonequilibrium state.

The answer can be found in an examination of the axial temperature profile along the boiler, as shown in Figure 3*b*. Associated with the pressure drop through the boiler, there is a corresponding decrease in saturation temperature from inlet to outlet. With net vapor generation, both the quality and the differential drop increases toward the exit end of the boiler, so that the axial profile of the saturation temperature is concave downward as shown in the figure. In accordance with the second law of thermodynamics, the inside wall temperature must be greater than the saturation temperature at any axial position, as shown by the dotted curve in Figure 3*b*. If the two-phase fluid enters the boiler at equilibrium then the vapor temperature at the boiler entrance would be equal to the saturation temperature. As the vapor flows through the boiler it sees a cooler liquid annulus and must necessarily give up sensible heat, cooling as it flows through the boiler. Where there is high slip and high vapor velocity, it is conceivable that the vapor reaches the measurement point from an upstream higher temperature point before it can reach equilibrium with the local temperature. The vapor temperature profile for this case would then rise from the saturation temperature in the vicinity of the liquid interface through a boundary layer to some superheat value represented by T_o in the central core. This would account for the observed inverse temperature profile for boiling two-phase flow by associating heat transfer from the wall to the liquid annulus with nonequilibrium cooling of the vapor core. The heat transferred to the liquid is converted into latent heat by bubble nucleation and growth and/or by evaporation at the liquid-vapor interface.

Factors which could be expected to enhance this nonequilibrium effect are high pressure drop through the boiler, a steep vapor temperature-pressure curve, high slip, high vapor velocity, and high liquid thermal conductivity. Factors which would tend to diminish this nonequilibrium effect are liquid entrainment in the vapor core, increased turbulent mixing, destruction of the annular flow pattern, and increased vapor thermal conductivity. The existence and degree of the nonequilibrium, inverse temperature profile are then governed by a balance of these various factors. The properties of alkali metals uniquely satisfy the conditions which enhance this nonequilibrium effect. Thus, comparing potassium to water at 1 atm. pressure, the vapor pressure curve of potassium is four times steeper than that of water,

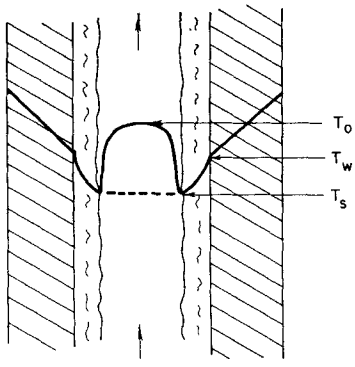

Fig. 3*a*. Radial and axial temperature profile for boiling two-phase flow.

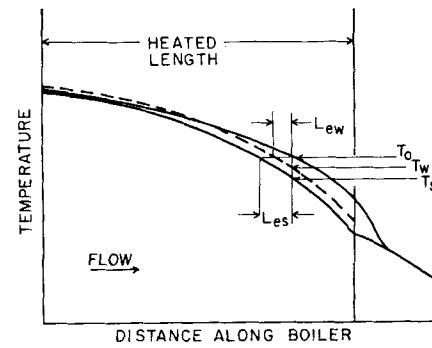

Fig. 3*b*. Radial and axial temperature profile for boiling two-phase flow.

(*Continued from page 1146*)

Direct contact heat transfer with change of phase: Condensation of single bubbles in an immiscible liquid medium. Preliminary studies, Sideman, Samuel, and Gideon Hirsch, **A.I.Ch.E. Journal, 11,** No. 6, p. 1019 (November, 1965).

Keywords: Heat Transfer-8, 7, Condensation-8, Bubbles-9, Liquid-9, Immiscible-0, Heat Transfer Coefficient-8, Isopentane-1, Alkanes-1, Water-5, Diameter-6, 7, Movie Camera-10, Velocity-6.

Abstract: Movie camera studies of single isopentane bubbles rising in still water yielded instantaneous heat transfer coefficients. But for the effect of bubble diameter, the results are similar to those of single drops evaporating in still water, indicating the similarity of the basic heat transfer mechanisms.

Stresses in a viscoelastic fluid in converging and diverging flow, Adams, E. B., J. C. Whitehead, and D. C. Bogue, **A.I.Ch.E. Journal, 11,** No. 6, p. 1026 (November, 1965).

Key Words: Shear Stress-8, Normal Stress-8, Stresses-8, Fluid-9, Non-Newtonian-0, Viscoelasticity-8, Flow-9, Converging-0, Diverging-0, Straight-0, Birefringence-8, Polystyrene-9, Aroclor-5.

Abstract: Birefringent studies have been carried out on a viscoelastic fluid (polystyrene in Aroclor) flowing in straight, in converging, and in diverging channels, for the purpose of obtaining point-by point stress data (the shear stress and the difference in normal stresses). A preliminary analysis in terms of the Coleman-Noll second-order theory for viscoelastic fluids shows good agreement.

Confined wakes: A numerical solution of the Navier-Stokes equations, Paris, Jean, and Stephen Whitaker, **A.I.Ch.E. Journal, 11,** No. 6, p. 1033 (November, 1965).

Key Words: A. Navier-Stokes Equation-8, 9, Wake-9, Flow-9, 8, Poiseuille Flow-9, Boundary Layer-9, Solution-8, Finite-Difference Equations-10.

Abstract: A numerical solution of the two-dimensional Navier-Stokes equations is presented for the confined wake formed by the merging of two plane Poiseuille flow streams. The system of finite-difference equations for the stream function and vorticity is solved by the Peaceman-Rachford elimination method for Reynolds numbers of 1, 50, 387, and 647.

At high Reynolds numbers, the primary boundary-layer simplification is imposed to yield a set of parabolic equations for the vorticity and stream function. The method outlined here represents an approximate solution for high Reynolds numbers, which gives surprisingly good agreement with the complete solution.

Analysis and design of gas flow reactors with application to hydrocarbon pyrolysis, Trombetta, Michael L., and John Happel, **A.I.Ch.E. Journal 11,** No. 6, p. 1041 (November, 1965).

Key Words: A. Analysis-8, 7, Design-8, 7, Reactors-9, Pyrolysis-4, Hydrocarbons-1, Temperature-6, Concentration-6, Mathematical Models-8, Differential Equation-10, Computer-10.

Abstract: This paper presents an approximate method of analysis of gas flow reactors which accounts for the effects of temperature and concentration gradients. The problem is reduced to the solution of a set of ordinary differential equations, which are integrated numerically. The result is a set of graphs giving correction factors to be applied to plug flow kinetic constants and reactor lengths. Although the primary interest is in hydrocarbon pyrolysis systems, the integral method graphs are applicable to other reaction systems.

(*Continued on page 1150*)

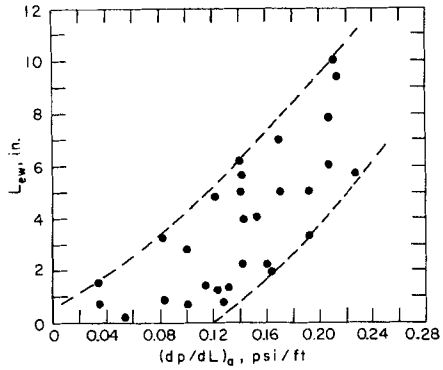

Fig. 4. Equilibrium distances.

slip ratios in two-phase flow have been measured to be orders of magnitude higher for potassium than for water (3), vapor velocities at the same total flow rate and at the same quality are much greater for potassium, and the liquid thermal conductivity of potassium is forty-five times that of water. It is likely due to these factors that the inverse temperature profile phenomenon has not been reported in earlier experiments with two-phase boiling flow of water. Heretofore, other experiments with boiling liquid metals have not attempted to measure the fluid core temperature and so were not able to observe this effect.

The superheat difference between T_o and T_w or T_s represents some equilibrium distance as illustrated in Figure 3*b*. This equilibrium distance has been calculated for the data and is plotted in Figure 4 as a function of acceleration pressure drop in the boiling test section. There appears to be a trend for increasing equilibrium distance with increasing pressure drop, as would be expected. For an average equilibrium distance of approximately 5 in. The vapor residence time was calculated to be of the order of 1 to 2 msec. This short time supports the assumption that the vapor can travel from an upstream point to the measurement point before it reaches equilibrium with the local temperature.

This nonequilibrium, inverse temperature profile is felt to be sufficiently different from the normally assumed picture heretofore and that it can have an important bearing on the understanding and general theory of convective boiling. Further efforts to check and document this phenomenon are under way.

LITERATURE CITED

1. Baker, R. A., and Alexander Sesonske, *Nucl. Sci. Eng.*, 13, No. 3 (1962).
2. Dwyer, O. E., *A.I.Ch.E. J.*, 9, 261 (1963).
3. Smith, L. R., Ph.D. dissertation, Univ. Michigan, Ann Arbor (1964).